Low temperature fluorescence imaging of freeze-trapped human cervical tissues

Nirmala Ramanujam
Department of Biomedical Engineering, University of Wisconsin, Madison, WI

Rebecca Richards-Kortum, Sharon Thomsen
Biomedical Engineering Program, University of Texas, Austin, TX

Anita Mahadevan-Jansen
Dept. Biomedical Engineering, Vanderbilt University, Nashville, TN

Michele Follen
Dept. Gynecologic Oncology, University of Texas, MD Anderson Cancer Center, Houston, TX

Britton Chance
Dept. Biochemistry and Biophysics, University of Pennsylvania, Philadelphia, PA

Abstract: We characterized the fluorescence intensity distribution within the epithelia and stroma of frozen human cervical tissues at the following excitation-emission wavelength pairs: 440, 525 nm and 365, 460 nm. The intensities at both excitation-emission wavelength pairs are significantly lower in the epithelia of severely dysplastic tissues, relative to that in normal and inflammatory tissues. Furthermore, there are small differences in (1) the epithelial intensity of severe dysplasia and mild dysplasia at 440, 525 nm and (2) the stromal intensity of inflammatory and severely dysplastic tissues at 365, 460 nm. A comparison of the ratio of intensities at 440, 525 nm and 365, 460 nm between the epithelia of each tissue type indicates that this ratio is lowest in severely dysplastic tissues. It is interesting to note that the epithelial and stromal intensities are comparable at 365, 460 nm; however, at 440, 525 nm, the epithelial intensity is more than a factor of two less that that of the stroma for all tissue types.

OCIS codes: (170.6280) Spectroscopy, fluorescence and luminescence; (170.6510) Spectroscopy, tissue diagnostics

References and Links

1. G.A. Wagnieres, W.M. Star and B.C. Wilson, "In vivo fluorescence spectroscopy and imaging for oncological applications," Photochem. Photobiol. **68**, 603-632 (1998).
2. R. Richards-Kortum and E. Sevick-Muraca, "Quantitative optical spectroscopy for tissue diagnosis," Ann. Rev. Phys. Chem. **47**, 555-606 (1996).
3. N. Ramanujam, " Fluorescence spectroscopy of neoplastic and non-neoplastic tissues," Neoplasia **2**, 1-29 (2000).
4. A. Pradhan, P. Pal, G. Durocher, L. Villeneuve, A. Balassy, F. Babai, L. Gaboury, L. Blanchard, "Steady state and time resolved fluorescence properties of metastatic and non-metastatic malignant cells from different species," J. Photochem. Photobiol. B: Biol. **31**, 101-112 (1995).
5. M. Anidjar, O. Cussenot, J. Blais, O. Bourdon, S. Avrillier, D. Ettori, J.M. Villter, J. Fiet, P. Teillac, A. Le Duc, "Argon laser induced autofluorescence may distinguish between normal and tumor human urothelial cells: a microspectrofluorimetric study," J. Urol. **155**, 1771-1774 (1996).
6. T.J. Romer, M. Fitzmaurice, R.M. Cothren, R. Richards-Kortum, M.V. Sivak Jr, J.R. Kramer Jr, "Laser-Induced fluorescence microscopy of normal colon and dysplasia in colonic adenomas: implications for spectroscopic diagnosis," Amer. J. Gastroenterol. **90**, 81-87 (1995).
7. G.S. Fairman, M.H. Nathanson, A.B. West, L.I. Deckelbaum, L. Kelly, C.R. Kapadia, "Differences in laser-induced autofluorescence between adenomatous and hyperplastic polyps and normal colonic mucosa by confocal microscopy," Digest. Dis. Sci. **40**, 1261-1268 (1995).

#30097 - $15.00 US Received January 03, 2001; Revised March 08, 2001

8. G. Bottiroli, A.C. Croce, D. Locatelli, R. Marchesini, E. Pignoli, S. Tomatis, C. Cuzzoni, S. Di Palma, M. Dalfante, P. Spinellu, "Natural fluorescence of normal and neoplastic human colon: a comprehensice "ex vivo" study," Lasers Surg. Med. **16**, 48-60 (1995).
9. F.N. Ghadially, W.J.P. Neish, H.C. Dawkins, "Mechanisms involved in the production of red fluorescence of human and experimental tumors," J. Path. Bact. **85**, 77-92 (1963).
10. B. Chance, N. Graham, V. Legallais, "Low temperature trapping method for cytochrome oxidase oxygen intermediates," Anal. Biochem. **67**, 552-579 (1975).
11. B. Chance, B. Schoener, R. Oshino, F. Itshak, Y. Nakase, "Oxidation-reduction ratio studies of mitochondria in freeze-trapped samples," J. Biol. Chem. **254**, 4764-4771 (1979).
12. B. Quistorff, J.C. Haselgrove, B. Chance, "High spatial resolution readout of 3-D metabolic organ structure: an automated, low-temperature redox ratio-scanning instrument," Anal. Biochem. **148**, 389-400 (1985).
13. L. Stryer, *Biochemistry* (W.H. Freeman and Company, 1988), Chap. 8.
14. C.K. Brookner, M. Follen, I. Boiko, J. Galvan, S.Thomsen, A. Malpica, S. Suzuki, R. Lotan, R.R. Richards-Kortum, "Autofluorescence patterns in short-term cultures of normal cervical tissue," Photochem. Photobiol. **71**, 730-736 (2000).
15. N. Ramanujam N, M.F. Mitchell, A. Mahadevan-Jansen, S. Thomsen, G. Staerkel, A. Malpica, T. Wright, A. Atkinson, R. Richards-Kortum, "Cervical pre-cancer detection using a multivariate statistical algorithm based on laser induced fluorescence spectra at multiple excitation wavelengths," Photochem. Photobiol. **64**, 720-735 (1996).
16. T.C. Wright, R.J. Kurman, A. Ferenczy, "Cervical Intraepithelial Neoplasia" in *Pathology of the Female Genital Tract*, A. Blaustein, ed. (Springer-Verlag, New York, 1994).
17. D. Fujimoto, "The structure of pyridinoline, a collagen crosslink," Biochem. Biophys. Res. Comm. **76**, 1124-1129 (1977).
18. J.P. Freyer, "Rates of oxygen consumption for proliferating and quiescent cells isolated from multicellular tumor spheroids," Adv. Exp. Med. Biol. **345**, 335-342 (1994).
19. U. Utzinger, E.V. Trujillo, E.N. Atkinson, M.F. Mitchell, S.B. Cantor, R. Richards-Kortum, "Performance estimation of diagnostic tests for cervical precancer based on fluorescence spectroscopy: effects of tissue type, sample size, population and signal-to-noise ratio," IEEE Trans. Biomed. **46**, 1293-1303 (1999).

1. Introduction

Steady-state fluorescence spectroscopy has been employed to provide fast and non-invasive detection of epithelial pre-cancers and cancers in a variety of organ sites, *in vivo*, including the colon, cervix and bronchus [1-3]. This technique has been shown to have a high sensitivity and specificity for discriminating between diseased and non-diseased tissue [1-3]. However, currently, there is a limited understanding of the specific biochemical and biophysical processes in tissue that lead to differences in the fluorescence spectra of diseased and non-diseased tissues. Hence, the diagnostically relevant information contained within a tissue fluorescence spectrum, has yet to be fully understood and exploited.

To date, several groups have elucidated to some extent, the fluorophores in epithelial tissues, which may give rise to differences in the fluorescence properties of normal tissues, pre-cancers and cancers. Particularly, fluorescence microscopy and micro-spectroscopy of micro-structures in cultured cells and optically thin, unstained, tissue sections have indicated that differences in the fluorescence spectra of normal, pre-cancerous and cancerous tissues may be attributed to differences associated with several endogenous fluorophores within the various sub-layers of these tissues. Pradhan et al. [4] showed that there is an increase in the fluorophores, reduced nicotinamide adenine dinucleotide (NADH) and tryptophan, while Anidjar et al. [5] reported a decrease in flavin adenine dinucleotide (FAD), as cells progress from a normal to cancerous state. Romer et al. [6] and Fairman et al. [7] observed a decrease in collagen fluorescence in pre-cancerous colon tissue sections, relative to that in normal colon tissue sections. Bottiroli et al. [8] observed a red fluorescence in some parts of a cancerous colon tissue section, a phenomenon, which has also been observed by others [9].

Although these investigations are insightful, there are several issues that have not been addressed in these studies. First, fluorescence microscopy and micro-spectroscopy of the unstained tissue sections were performed at room temperature. Chemical species associated with the metabolic pathway in tissue such as fluorescent NADH can be oxidized to non-fluorescent nicotinamide adenine dinucleotide (NAD^+) under these conditions. Second, the tissue vasculature is not intact in these unstained tissue preparations. Therefore the effect of

#30097 - $15.00 US Received January 03, 2001; Revised March 08, 2001

hemoglobin absorption is not represented. Hence, the fluorescence intensity distribution that is imaged from these unstained tissue slices using conventional fluorescence microscopy and micro-spectroscopy may be influenced by the tissue preparation and measurement conditions.

Chance et al. [10-12] have previously developed a method that can overcome to a large extent the aforementioned limitations; that is, this method can better preserve the intact tissue state for fluorescence imaging. Specifically, a tissue sample preparation method and an apparatus have been developed that enables high resolution (~50 μm), fluorescence imaging to be performed from rapidly-freeze trapped tissue blocks (rather than tissue slices) at liquid nitrogen temperatures [12]. First, aluminum tongs, pre-cooled in liquid nitrogen, are used to rapidly freeze-trap the tissue. Fluorescence images of the frozen tissue block are then obtained using an optical scanner with a stepper motor driven light guide, while the sample is immersed in liquid nitrogen [12]. The problem of optical coupling through the large temperature gradient is solved by the use of the light guide, the tip of which is placed in close proximity (50 μm) to the tissue surface. Chance et al. [10,11] have used this approach to perform high resolution, fluorescence imaging of NADH and FAD from freeze-trapped animal tissue blocks in various metabolic states.

The goal of this paper is to adapt the previously described approach to characterize the fluorescence of specific chemical species in human cervical tissues. Previous studies on fluorescence spectroscopy of cultured cells [4,5] have led us to hypothesize that there are differences in the fluorescence of NADH and FAD between normal, inflammatory and dysplastic cervical tissues. NADH and the reduced form of FAD, reduced flavin adenine dinucleotide ($FADH_2$) are the major electron carriers in the metabolic pathway [13]. These co-factors transfer their electrons to molecular oxygen by means of the electron transport chain. As a result, molecular oxygen oxidizes them to NAD^+ and FAD. Fluorescence measurements from a suspension of human cervical cancer cells indicates that NADH and FAD have an excitation-emission maxima of 350, 460 nm and 450, 520 nm, respectively [14]. The ratio of the fluorescence intensities of FAD (oxidized) and NADH (reduced) at their excitation-emission maxima gives a measure of the oxidation-reduction (redox) state of the tissue [11]. A decrease in the redox ratio of the tissue reflects an increase in the metabolic rate [11]. Hence, we hypothesize that there are differences in the metabolic activity of normal, inflammatory and dysplastic cervical tissues.

2. Methods

Fluorescence measurements of human cervical tissues were carried out *in vivo* and then, subsequently, *in vitro*. Specifically, fluorescence spectra of intact cervical tissues were measured at 337, 380 and 460 nm, excitation [15]. Tissues biopsies were then obtained from sites at which spectra were measured. These tissue samples were freeze-trapped in liquid nitrogen. Subsequently, high resolution, fluorescence images were obtained from cross-sections (perpendicular to the tissue surface) of these frozen tissue blocks at the following excitation-emission wavelength pairs: at 365 nm excitation and 460 nm emission (365, 460 nm) and at 440 nm excitation and 525 nm emission (440, 525 nm). These excitation-emission wavelength pairs are near the excitation emission maxima of NADH and FAD [14].

2.1 *In vitro studies*

A low temperature fluorometer, constructed at the Johnson Foundation of the University of Pennsylvania was used to image the fluorescence intensities from the cross-sectional surface of freeze-trapped tissue blocks and is described in detail elsewhere [12]. The low temperature fluorometer incorporates a liquid nitrogen sample chamber, a milling head, and an optical scanner (mercury arc lamp, photo multiplier tube, filters) with a stepper motor driven light guide. The frozen tissue (embedded in isopentane or other tissue embedding medium) is mechanically fixed in a chuck and then placed in the liquid nitrogen chamber. A flat tissue surface is created by low temperature milling of the tissue with a grinder. The tip of the light guide is then placed at a distance of 50 μm from an appropriate point on the tissue surface.

#30097 - $15.00 US Received January 03, 2001; Revised March 08, 2001

During operation, the light guide is stepped across the tissue surface at a fixed increment, and fluorescence measurements are made from each discrete site. In this study, the computer controlled scan size was 128 x 128 pixels, the step size of the light guide was 20 μm and each pixel was sampled every 16 ms and four sampled points were averaged per pixel. The low temperature fluorometer was used to measure fluorescence intensities at 365 nm excitation (40 nm bandpass) and 460 nm emission (50 nm bandpass) and at 440 nm excitation (20 nm bandpass) and 525 nm emission (50 nm bandpass).

After each tissue experiment, fluorescence measurements were made from the surface of a fused silica cuvette, which contained a homogeneous calibration standard (Black light pigment, blaze orange powder, Edmund Scientific, NJ), with the light guide at a fixed position and at a fixed distance (50 μm) from the cuvette wall. The fluorescence measurements from each pixel of the tissue surface were normalized to the corresponding measurement from the standard to account for day-to-day variations in the source intensity and gain settings.

The fluorescence images at 440, 525 nm and at 365, 460 nm were processed using the "NIH" image software. Also, a redox ratio index image was calculated for just the epithelial region of each tissue block. The redox ratio index image is defined as the ratio of the intensity at 440, 525 nm and the sum of the intensities at 440, 525 nm and 365, 460 nm (ratio lies between 0 – 1). In calculating the redox ratio index for the epithelium, it was assumed that the fluorescence at 440, 525 nm is due to FAD and that at 365, 460 nm is attributed to NADH. Therefore, the redox ratio index can also be defined as follows: redox ratio index = FAD/(FAD+NADH).

2.2 Animal and human tissue preparation

Two different types of tissues were evaluated in this study. First, fluorescence imaging was performed on rat liver tissues in various metabolic states, induced by carbogen, air and nitrogen inhalation. The purpose here was to establish the dynamic range of the redox ratio index in tissues. Second, fluorescence imaging was performed on normal, inflammatory and dysplastic human cervical tissues. The goal here was to determine if there are differences in the fluorescence and consequently, the redox ratio indices of these different tissue states.

Rat liver tissues. Male Wistar rats (Harlan Sprague Dawley, Inc., Indianapolis) weighing approximately 200 grams were used. These rats were housed individually with ad libitum access to food and water, and kept under controlled environmental conditions (22^{o}C, relative humidity 45-55%, 12 hour light / dark cycle). Animal care and procedures were in accordance with the guidelines in the U.S. department of Health and Human Services and National Institutes of Health "Guide for the Care and Use of Laboratory Animals" and approved by the Institutional Animal Care and Use Committee at the University of Pennsylvania.

The rats were divided into three groups: 10 rats (controls) underwent air inhalation, 8 rats underwent carbogen inhalation for 60 – 300 s to induce hyperoxia and 7 rats underwent nitrogen inhalation for 30 - 120 s to induce hypoxia. Each rat was anesthetized by intraperitoneal injection of sodium pentobarbitol (5 mg / 100 mg) and surgery was performed to expose the trachea and the liver. A tracheal cannula was employed so that gas inhalation could be administered. The gas flow rate was 1 liter / minute. In each group, after the gas inhalation, the liver tissue was freeze-clamped by pre-cooled aluminum tongs. The freeze-trapped tissue was stored in liquid nitrogen until the fluorescence measurements were made.

Human cervical tissues. Patient consent was obtained for the human cervical tissue fluorescence studies, which was reviewed and approved by the Institutional Review Boards of the University of Texas, MD Anderson Cancer Center. The average age of the patients who participated was 26 years $\pm$ 6.3. In general, a colposcopically appearing normal tissue and abnormal tissue were obtained from each patient. Each tissue was excised using a biopsy forceps, immediately placed in a small metal container on ice containing a tissue embedding medium (OCT), oriented such that the tissue surface was perpendicular to the surface of the embedding medium and then finally transferred with the metal container to liquid nitrogen.

#30097 - $15.00 US Received January 03, 2001; Revised March 08, 2001

The time duration between excision and placement of the tissue in OCT was approximately 30 seconds. The tissue with the metal container was then transferred from ice to liquid nitrogen within another 30 seconds and stored until the fluorescence measurements were made. After the fluorescence measurements, the tissue was submitted for histological evaluation. A serial section of the frozen tissue block was obtained using a tissue sectioning microtome and then stained with hemotoxylin and eosin (H&E).

Each H&E stained tissue section was evaluated by a board certified pathologist (ST) according to the World Health Organization (WHO) classification. Tissues were classified into one of the following categories: normal squamous, normal columnar, metaplasia, inflammation, human pappilloma virus (HPV) or dysplasia (mild, moderate or severe). If any of these tissues were characterized as having more than one disease state (for example, mild dysplasia and severe dysplasia), these samples were characterized by the most severe disease state. Fluorescence imagined from only 22 of the 30 tissue biopsies were retained for further analysis. The 8 tissue samples that were discarded had freezing artifacts in their corresponding H&E stained sections and therefore could not be diagnosed. Of the 22 remaining samples, nine were histologically classified as normal squamous, 6 had inflammation and 7 were dysplastic (3 mild dysplasias and 4 severe dysplasias). Only two of the 7 dysplastic tissues had a corresponding histologically normal tissue that was obtained from the same patient. Only three of the 6 samples with inflammation had a normal counterpart from the same patient.

In order to evaluate if the fluorescence and consequently, the redox ratio index of a tissue is affected if it is frozen after excision (human cervical tissue) rather than while it is intact (rat liver), an additional experiment was performed in which two liver lobes from the same rat were freeze-trapped using two different procedures. In the first case (*in vivo* freeze-trapping), the liver tissue was freeze-clamped by pre-cooled aluminum tongs. In the second case (*in vitro* freeze-trapping), the tissue was biopsied, placed within approximately 30 seconds in a metal container on ice, containing chilled isopentane and then transferred with the metal container within 30 seconds to liquid nitrogen. Both tissues were stored in liquid nitrogen until they were mounted and milled for the fluorescence measurements.

3. Results

Figure 1 displays the average redox ratio index of rat livers that underwent carbogen, air and nitrogen inhalation. In each tissue sample, the redox ratio index was calculated from a tissue area that was 1 mm^2. The redox ratio indices of all tissues that underwent a particular gas perturbation were then averaged. Evaluation of Fig. 1 indicates that the redox ratio index ranges from 0.5 - 0.32. The redox ratio index is highest for the livers of rats that underwent carbogen inhalation and lowest for the livers of those that underwent nitrogen inhalation, as would be expected. The redox ratio index of the un-perturbed livers was only slightly lower than that of the carbogen-perfused livers.

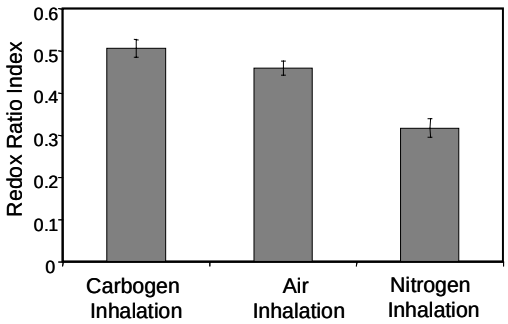

Fig. 1. Average redox ratio index of rat livers that underwent carbogen, air and nitrogen inhalation

#30097 - $15.00 US Received January 03, 2001; Revised March 08, 2001

Table 1 provides the fluorescence intensities at 460, 525 nm, 365, 460 nm and the corresponding redox ratio indices of two rat liver tissues that underwent *in vivo* and *in vitro* freeze-trapping, respectively. For each tissue sample, the mean and standard deviation of the fluorescence intensities and the redox ratio index were calculated from an area of liver tissue that was 1 mm^2. Note that the fluorescence intensities are indicated on an 8 bit scale (0 – 255) while the redox ratio index is indicated on a scale between 0 – 1. A comparison of the fluorescence intensities as well as the redox ratio index of the two rat liver tissues that underwent different freezing protocols indicates that they are very similar. This experiment is a necessary precedent to low temperature fluorescence imaging of human cervical tissues.

Table 1. Fluorescence intensities at 460, 525 nm, 365, 460 nm and the redox ratio indices of two rat liver tissues (from the same rat) that underwent *in vivo* and *in vitro* freeze-trapping, respectively

Liver Tissue	I(440, 525 nm) FAD	I(365, 460 nm) NADH	Redox Ratio Index FAD/(FAD+NADH)
In vivo freeze-trapping	128.8 ± 26	128.6 ± 12	0.54 ± 0.01
In vitro freeze-trapping	120.5 ± 24	122.1 ± 13	0.53 ± 0.02

Figure 2 displays a H&E stained section of a normal cervical tissue and the corresponding fluorescence images at the two excitation-emission wavelength pairs: 440, 525 nm and 365, 460 nm. The H&E stained tissue section consists of a superficial epithelium and an underlying stroma [16]. The two regions are separated by a basement membrane. The corresponding fluorescence images are congruent with the H&E stained tissue section and their color intensity scale ranges from a minimum of zero denoted by black to a maximum of 255 denoted by white. An increase in the color intensity scale corresponds to an increase in the fluorescence intensity. The black outline in the images demarcates the epithelium from the stroma. This was determined by superposing the fluorescence images onto the H&E stained tissue image. At 365, 460 nm, the fluorescence in the epithelium arises from NADH in epithelial cells; the fluorescence from the stroma may have contributions from NADH in the fibroblasts and from the collagen fibers (excitation-emission maxima of collagen is 325, 390 nm) [17]. At 440, 525 nm, the fluorescence is primarily attributed to that of FAD. Evaluation of Fig. 2 indicates that the fluorescence intensity at 440, 525 nm is lower in the epithelium relative to that in the underlying stroma, while the opposite trend is observed at 365, 460 nm.

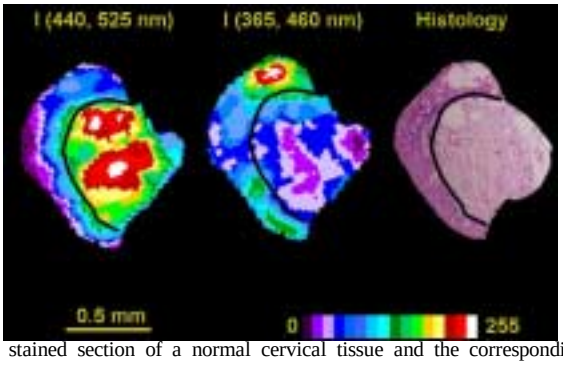

Fig. 2. H&E stained section of a normal cervical tissue and the corresponding fluorescence images at two excitation-emission wavelength pairs: 440, 525 and 365, 460 nm.

Figure 3 displays the average fluorescence intensity as a function of tissue depth at (a) 440, 525 nm and (b) 365, 460 nm for a normal, inflammatory and severely dysplastic tissue. Intensity versus depth was averaged over an image area selected perpendicular to the basement membrane. The width of the selected area was chosen to be as wide as possible and is on average, 2000 μm. The depth was fixed at 1500 μm. Evaluation of Fig. 3(a) indicates that the intensity at 440, 525 nm is significantly greater in the stroma, relative to that in the

#30097 - $15.00 US Received January 03, 2001; Revised March 08, 2001

epithelium for all three-tissue types. Additionally, in the stromal region, the intensity of the severely dysplastic tissue is significantly more heterogeneous as a function of depth compared to the normal tissue and the tissue with inflammation. Examination of Fig. 3(b) indicates that the intensity at 365, 460 nm is similar in the epithelium and stroma for tissues with inflammation and severe dysplasia; however, in the case of the normal tissue, the intensity in the stroma is less than that in the epithelium. The redox ratio index image is not shown in Fig. 2 because this ratio may not be valid for the stromal region where collagen fluorescence could contaminate the NADH fluorescence at 365, 460 nm.

Figure 4 displays the average fluorescence intensity at 440, 525 nm and 365, 460 nm for (a) the epithelium and (b) the stroma of normal, inflammatory, mildly dysplastic and severely dysplastic tissues. The average intensities of the epithelium and stroma of each tissue sample were calculated from the corresponding intensity-depth image and then averaged for all samples within a tissue type. In Fig. 4(a), the intensity at 440, 525 nm of severely dysplastic tissue epithelia is less than that of the other three tissue types; at 365, 460 nm, the severely dysplastic tissue intensity is less than that of normal and inflammatory tissues. In Fig. 4(b), the intensity at 440, 525 nm is similar for the stroma of all four-tissue types; at 365, 460 nm, there are small differences in the intensity of inflammation and severe dysplasia.

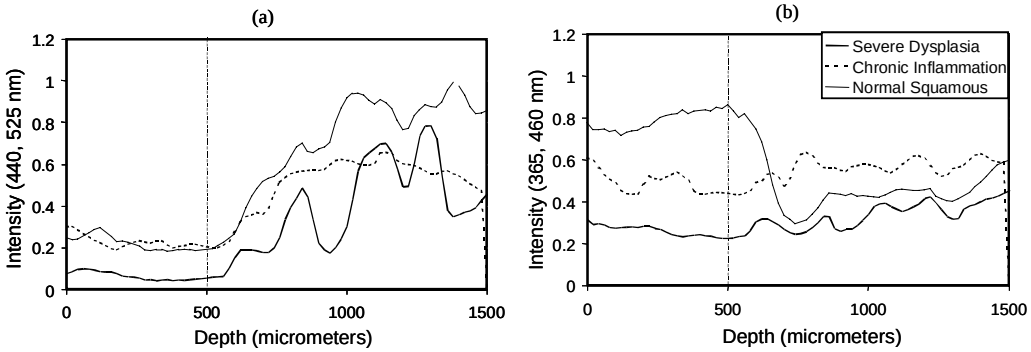

Fig. 3. The average fluorescence intensity as a function of tissue depth at (a) 440, 525 nm and (b) 365, 460 nm for a normal, inflammatory and severely dysplastic tissue.

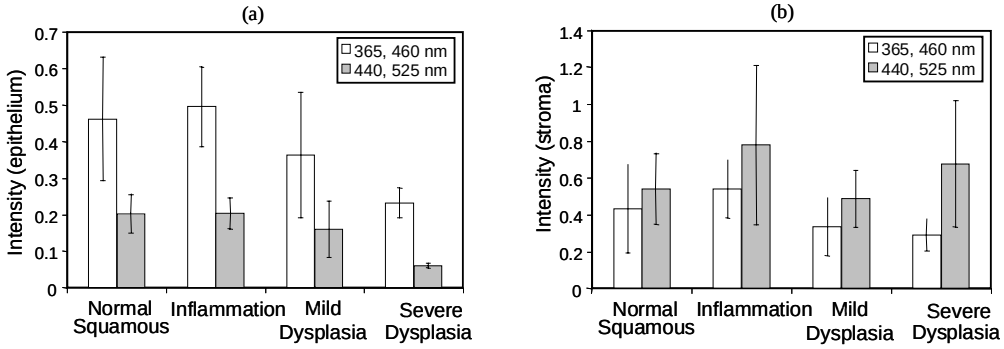

Fig. 4. Average fluorescence intensity at 440, 525 nm and 365, 460 nm for (a) the epithelium and (b) the stroma of normal, inflammatory, mildly dysplastic and severely dysplastic tissues.

Figure 5 displays the (a) average redox ratio index of the epithelia and (b) average ratio of the epithelial and stromal intensity at 440, 525 nm and 365, 440 nm of the four different tissues. The redox ratio and the epithelial-stromal intensity ratio was obtained for each tissue and then averaged for all samples within a tissue type Fig. 5(a) indicates that the redox ratio index is similar in normal, inflammation and mild dysplasia but significantly lower in severe dysplasia. The redox ratio was not calculated for the stroma due to the potential contribution

#30097 - $15.00 US Received January 03, 2001; Revised March 08, 2001

of collagen fluorescence at 365, 460 nm. Fig. 5(b) indicates that the epithelial-stromal intensity ratio is between 0.1-0.4 at 440, 525 nm, and between 0.8-1.2 at 365, 460 nm.

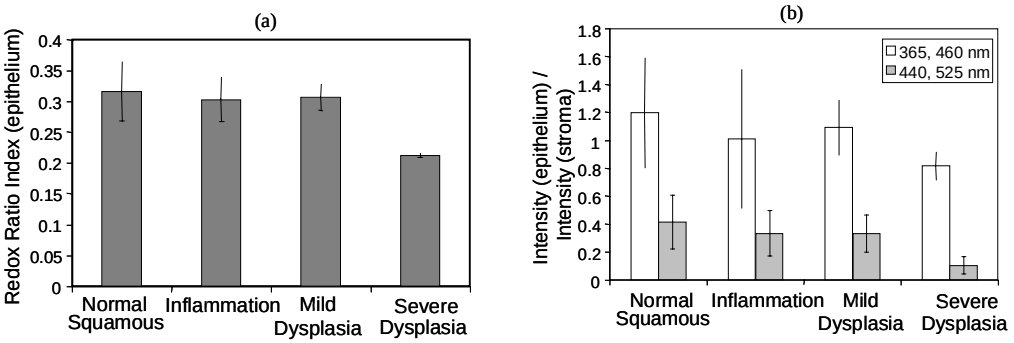

Fig. 5. The (a) average redox ratio index of the epithelia and (b) average ratio of the epithelial and stromal fluorescence intensity at 440, 525 nm and 365, 440 nm of the four different tissues.

4. Discussion and conclusions

The goal of the study described in this article was to characterize the fluorescence of specific chemical species in human cervical tissues. Specifically, this study tested the hypothesis that there are differences in the redox ratio index of normal, inflammatory and dysplastic cervical tissues. The results from high resolution, low temperature fluorescence imaging of freeze-trapped cervical tissues indicates that there are differences in fluorescence intensity of severely dysplastic tissues and the other three tissue types. Specifically, the intensities at 440, 525 nm and 365, 460 nm are significantly lower in the epithelia of severely dysplastic tissues, relative to that in normal and inflammatory tissues. Furthermore, there are small differences in (1) the epithelial intensity of severe dysplasia and mild dysplasia at 440, 525 nm and (2) the stromal intensity of inflammatory and severely dysplastic tissues at 365, 460 nm. A comparison of the redox ratio index between the epithelia of each tissue type indicates that this ratio is lowest in severely dysplastic tissues. A decrease in the redox ratio index suggests an increase in the metabolic rate. An increase in the metabolic rate seems logical since at least some proportion of the dysplastic cells are undergoing rapid cell division [18]. It should be pointed out that only four severely dysplastic tissue samples were evaluated in this study. Therefore, a larger sample size is required to confirm these initial findings. Additionally, it is interesting to note that the epithelial and stromal intensities are comparable at 365, 460 nm; however, at 440, 525 nm, the epithelial intensity is more than a factor of two less that that of the stroma for all tissue types. Another point to note is that all the analysis done in this work was unpaired, that is, the fluorescence properties of normal, inflammatory and dysplastic tissues from different patients were compared. A paired analysis in which the fluorescence properties of a normal, inflammatory and dysplastic tissue are compared within a patient may yield additional differences that are not readily observed in the unpaired analysis.

Utzinger et al. [19] have analyzed the performance of multivariate statistical algorithms, which employ different combinations of fluorescence spectra at 337, 380 and 460 nm excitation to differentiate (1) dysplasia from normal tissue and (2) moderate / severe dysplasia from mild dysplasia and normal tissues of the human cervix. They found that when they used spectra at only single excitation wavelengths in the algorithm, the spectra at 460 nm excitation were always more effective in discriminating between the two pairs of tissue types than spectra at 380 nm excitation. This is consistent with the results in Fig. 4(a), which show that the greatest differences in the epithelial intensity of severe dysplasia and normal tissues and severe dysplasia and mild dysplasia occur at 440 nm excitation. Although Utzinger et al. did not include tissues with inflammation in their analysis our study does indicate that it is possible to discriminate between severe dysplasia and inflammation at both 440, 525 and 365,

#30097 - $15.00 US Received January 03, 2001; Revised March 08, 2001

460 nm. No differences were observed between mild dysplasia and inflammation at these excitation-emission wavelength pairs.

Brookner et al. [14] have imaged the fluorescence intensity distribution of normal human cervical tissue cultures of women in different age groups. In their study, fluorescence images were obtained at 380 and 455 nm excitation, which are similar to those used in our investigation. At an excitation wavelength of 380 nm, they integrated the fluorescence at wavelengths greater than 397 nm. At an excitation wavelength of 455 nm, the fluorescence was integrated at wavelengths greater than 495 nm. An analysis of the fluorescence images that they obtained indicates that the ratio of the epithelial and stromal intensity decreases with increasing age (group 1: 30.9 years, group 2: 38 years and group 3: 49.2 years). Furthermore, for the youngest age group of 30.9 years (11 subjects), the epithelial-stromal intensity ratio is slightly greater than 1 (~1.2) at 380 and 460 nm excitation. In our study, the normal tissues that were studied were obtained from a total of 9 patients and the average age of this group was 26 years $\pm$ 7.5. Because of the similarities between the youngest age group studied by Brookner et al. [14] and the age group in our study, we decided to compare our results to theirs. A comparison of the results at 365 (our study) and 380 nm excitation indicates that the epithelial-stromal intensity ratios are very similar (~1.2). However, a comparison of the results at 440 (our study) and 455 nm excitation indicates that the epithelial-stromal intensity ratio obtained from our study is a factor of three less than that reported by Brookner et al [14]. The discrepancy in the second set of results may be attributed to the tissue preparation protocol, the tissue sample studied, the temperature and the excitation wavelengths at which fluorescence measurements were made.

#30097 - $15.00 US Received January 03, 2001; Revised March 08, 2001